Chance-Constrained Optimization for Multi Energy Hub Systems in a Smart City

Da Huo, Chenghong Gu, *Member, IEEE*, Kang Ma, *Member, IEEE*, Wei Wei, Yue Xiang, *Member, IEEE*, and Simon Le Blond

***Abstract*— The Energy Hub is a powerful conceptualisation of how to acquire, convert, and distribute energy resources in the smart city. However, uncertainties such as intermittent renewable energy injection present challenges to energy hub optimization. This paper solves the optimal energy flow of adjacent energy hubs to minimize the energy costs by utilizing the flexibility of energy resources in a smart city with uncertain renewable generation. It innovatively models the power and gas flows between hubs using chance constraints, thus permitting the temporary overloading acceptable on real energy networks. This novelty not only ensures system security but also helps reduce or defer network investment. By restricting the probability of chance constraints over a specific level, the energy hub optimization is formulated as a multi-period stochastic problem with the total generation cost as the objective. Cornish-Fisher Expansion is utilized to incorporate the chance constraints into the optimization, which transforms the stochastic problem into a deterministic problem. The interior-point method is then applied to resolve the developed model. The proposed chance-constrained optimization is demonstrated on a 3-hub system and results extensively illustrate the impact of chance constraints on power and gas flows. This work can benefit energy hub operators by maximizing renewable energy penetration at the lowest cost in a smart city.**

***Index Terms*—Chance-Constrained Programming, Cornish-Fisher Expansion, Energy Hub, Optimal Flow**

I. Introduction

A smart energy city enables flexible management of energy infrastructure to efficiently meet demand. Within a smart energy city, the energy hub concept can coordinate multiple energy carriers to optimally satisfy demand [1-5]. Energy hubs could increase energy system flexibility and exploit the unused capacity of various energy carriers. Energy hubs have been applied to many energy system planning and operation problems in smart energy cities, such as demand response [6], system operations [7], and optimal power flows [8]. Buildings or communities in the smart energy city can be treated as energy hubs [1, 9] and the energy flows between them can be optimally scheduled to minimize energy transportation and exploitation costs, minimizing the energy costs of a smart energy city. The optimal energy flow of energy hub involves optimizing electricity and other carriers, such as natural gas and heat, which can be formulated as a multi-period problem. In [10-13], the optimization for multi-carrier systems including adjustment of the energy flows between hubs is investigated.

In the aforementioned literature, the steady-state model of energy hub systems is utilized and optimization problems are all formulated as deterministic models. In reality, uncertainties always present in energy management, due to customer load and renewable energy. System thermal and voltage constraints may be temporarily violated if uncertain variables are underestimated, otherwise system operational cost will be prohibitively high when the impact of uncertain variables is overestimated [14]. Therefore, modelling and estimation of uncertain variables are important in optimizing energy hubs.

Uncertainty has been included in energy hub optimization in previous research. In [5, 15, 16], Monte Carlo simulation is applied to model the uncertain inputs but the optimization requires much computational effort due to the large number of scenarios. A scenario reduction method is applied to minimise the number of scenarios in [17, 18]. Other methods including two-point estimate method (2PEM), the point estimate method, and the improved 2PEM method have been applied in [19-21] respectively to model renewable generation in energy hub systems. The reality is that a certain number of scenarios may not completely represent the stochastic nature of uncertain variables, causing the results to be inaccurate.

In contrast to scenario-based methods, chance-constrained programming (CCP) is a consistently robust and reliable approach to resolve uncertainty [22]. Each chance constraint is modelled by a boundary, the acceptable probability of constraint violation. The CCP optimization is then resolved to meet both normal constraints and chance constraints. Whilst the stochastic nature of uncertain elements can cause occasional system overloading, investment to meet these rare stress events could be prohibitively expensive. However, in reality, some temporary overloading is tolerable in both gas and electricity networks, and CCP is, therefore, a promising approach to this problem. CCP has been applied to power system operating problems, including demand response, optimal power flow, and

Manuscript received October 18, 2017; revised January 28, 2018, April 23, 2018, and June 14, 2018; accepted July 21, 2018.

D. Huo, C.Gu (corresponding author), K. Ma, W. Wei, and S.L. Blond are with the Department of Electronic & Electrical Engineering, University of Bath, Bath, UK (e-mail: dh466@bath.ac.uk; c.gu@bath.ac.uk; k.ma@bath.ac.uk; w.wei@bath.ac.uk; s.p.leblond@bath.ac.uk).

Y. Xiang is with the College of Electrical Engineering and Information Technology, Sichuan University, Chengdu, China, (e-mail: exxyye@gmail.com).

unit commitment [23], [24], and [25]. However, it has not been applied to the energy hub optimization problem.

This paper formulates a novel, chance-constrained approach to solve the optimal energy flows for multiple energy hubs with uncertain renewable generation. The uncertain elements of solar and wind generations are simulated by fitting historical data to specific distributions. The power and gas flows along branches between adjacent hubs are modelled as chance constraints at specific probability levels. The optimization thus becomes a non-convex stochastic problem. In solving the CCP problem, the non-convex CCP problem is converted into a convex problem and linear programming is applied in [26]. The back-mapping approach is utilized in [22, 24], where the probability of chance constraints is derived by mapping them back to the uncertainty variables' distributions. Non-linear programming is then applied to solve the optimization problem. A sample average approximation method is developed in [27] to resolve chance-constrained problems.

This paper utilizes the Cornish-Fisher Expansion method to translate chance constraints into deterministic constraints so that deterministic programming can be applied. Because of its flexibility and robustness [1], the interior point method is thus used to solve the developed model. The CCP enables energy hub system reliability to be realized above a specific level with low costs by restricting the probability of the chance constraints over the predefined level. This work can benefit energy hub operators by maximizing renewable energy penetration at the lowest cost in a smart city.

The main contributions of the paper are as follows: i) compared with [24] where the load uncertainties are modelled as random inputs in multiple hub optimization, the uncertainty of renewable generation is considered in multi-hub optimization; ii) in contrast to only treating the power flows between buses as chance constraints [24], both power and gas flows between adjacent hubs are restricted by chance constraints; iii) the CCP is incorporated into the energy hub optimization, which can better model the uncertainty characteristics compared with the scenario generation methods in [17-21] and reduce the huge computational burden caused in [5, 15, 16]; iv) in contrast to the approaches in [22, 24, 26, 27] for solving CCP, the chance constraints are mathematically converted into deterministic constraints through Cornish Fisher Expansion, and thus the deterministic programming is applied to solve CCP; v) the impact of chance constraints on energy hub system optimization is extensively investigated; vi) the comparison between CCP and deterministic approaches is quantified by using the value of expected value of perfect information (EVPI) and value of the stochastic solution (VSS) .

The remainder of the paper is organised as follows: the mathematical formulations of the energy hub system with the power and gas network are illustrated in section II. The CCP problem formulation and the methodology of implementing the CCP for the system optimization are introduced in section III. Section IV introduces the concepts of EVPI and VSS. Section V discusses different case studies and related results, and section VI concludes the paper.

II. Energy Hub System Modelling

The mathematical model of the energy hub system is illustrated in this section. The equality constraints are based on the law of energy conservation between hubs. The inequality constraints arise from safe operational limits such as maximum converter output and maximum power injection to a single hub.

A. Energy Hub

Both electricity and heat demand can be satisfied by adjusting different energy converters in hubs according to optimization objectives. The energy hub used in this paper is equipped with energy converters, namely Combined Heat and Power (CHP), Ground Source Heat Pump (GSHP), and Gas Furnace (GF). CHP simultaneously generates heat and power, GF combusts gas to generate heat. GSHP coverts power to heat by extracting heat from the ground, and it is widely used in Europe and American due to its high efficiency.

The relations between converter inputs and outputs for CHP, GSHP, and GF are shown in (1), (2), and (3) respectively. η_e and η_{gh} indicate the electric and thermal efficiency of CHP. The efficiency of GSHP is the coefficient of performance (COP). η_F is the efficiency of GF. P_{CHP}, P_{HP}, and P_{GF} represent the energy injection to CHP, GSHP, and GF. The electric output $P_{CHP,Eout}$ and heat output $P_{CHP,Hout}$ of CHP are quantified by (1a) and (1b), the outputs of GSHP $P_{HP,out}(t)$ and GF $P_{GF,out}(t)$ are calculated by (2) and (3).

$$P_{CHP,Eout}(t) = \eta_e \cdot P_{CHP}(t) \quad (1a)$$

$$P_{CHP,Hout}(t) = \eta_{th} \cdot P_{CHP}(t) \quad (1b)$$

$$P_{HP,out}(t) = COP \cdot P_{HP}(t) \quad (2)$$

$$P_{GF,out}(t) = \eta_F \cdot P_{GF}(t) \quad (3)$$

Heat storage is also considered to store excessive heat, which can be utilized later when the heat load is exorbitant. Heat storage is formulated in (4) [28], where M_h specifies the energy exchange between the hub and heat storage, E_h indicates the stored energy, and E_h^{stb} is the standby thermal loss through the water tank wall at the current time interval. e_h^+ and e_h^- are the charging and discharging efficiency respectively. These variables are a function of t, denoting the time step within a discretized time domain.

$$M_h(t) = \frac{1}{e_h}\left(E_h(t) - E_h(t-1) + E_h^{stb}\right) \quad (4a)$$

$$e_h = \begin{cases} e_h^+ & \text{if } M_h(t) \geq 0 \quad \text{(charging/standby)} \\ \frac{1}{e_h^-} & \text{else} \qquad\qquad\qquad \text{(discharging)} \end{cases} \quad (4b)$$

Because the storage charges when M_h is greater than 0, the above equation means: the stored energy at current time step *t* equals the stored energy at previous time step *(t-1)* plus the charging energy multiplied by the charging efficiency, minus the standby loss. This explanation also applies when the storage discharges.

Additionally, renewable generation including solar photovoltaics and wind generation cooperates with other hub elements to meet demand. The output of the solar photovoltaic system $P_{so,out}$ is quantified by multiplying solar irradiance $P_{so,in}$ with the efficiency η_{so}.

$$P_{so,out} = P_{so,in} \cdot \eta_{so} \quad (5)$$

The power output P_{wi} from wind turbines is expressed in terms of the wind speed v_w (m/s) as shown in (6) [29], where v_{ci},

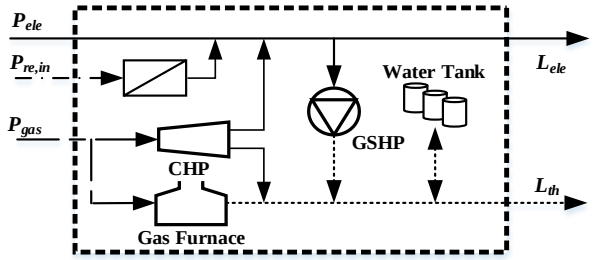

Fig. 1. Single energy hub

v_{rs}, and v_{co} represents the cut-in, rated, and cut-out wind speed, P_{rated} indicates the rated power.

$$P_{wi} = \begin{cases} 0, & \text{if } 0 < v_w < v_{ci}, \text{or } v_w > v_{co} \\ P_{rated} \cdot \left(\frac{v_w - v_{ci}}{v_{rs} - v_{ci}}\right), & \text{if } v_{ci} \le v_w \le v_{rs} \\ P_{rated}, & \text{if } v_{rs} \le v_w \le v_{co} \end{cases} \quad (6)$$

The energy hub modelled represents a community such as a university or hospital in a smart energy city. The schematic diagram of a single energy hub is shown in Fig. 1.

As indicated in Fig. 1, the demand including electricity L_{ele} and heat L_{th} is satisfied by electricity input P_{ele}, gas input P_{gas}, energy exchange with the storage M_h, and renewable generation $P_{re,in}$. The energy hub system presents multiple inputs and outputs, hence the coupling between hub outputs (represented as L) and inputs (represented as P) is formulated with a matrix of converter efficiencies (representing as C). The mathematical transformation of the energy hub in Fig. 1 is formulated in (7).

$$\begin{bmatrix} L_{ele}(t) \\ L_{th}(t) + M_h(t) \end{bmatrix} = \begin{bmatrix} 1 - v_e(t) & \eta_{re}(1 - v_e(t)) & v_g(t)\eta_e(1 - v_e(t)) \\ v_e(t)COP & v_e(t)\eta_{re}COP & v_g(t)\left(\eta_{gh} + \eta_e v_e(t)COP\right) + \eta_F - v_g(t)\eta_F \end{bmatrix} \times \begin{bmatrix} P_{ele}(t) \\ P_{re,in}(t) \\ P_{gas}(t) \end{bmatrix} \quad (7)$$

As indicated in (7), v_e and v_g are the dispatch factors of electricity and gas. Specifically for this hub, v_e indicates the portion of electricity injection to GSHP relative to the total electricity input. Similarly, v_g is the proportion of gas injected to CHP relative to the total gas input.

B. Electricity Networks

The mathematical formulations of electricity networks are indicated as follows [8]. The complex nodal power balance for node m is in (8), where S_m is the complex power injected to node, S_{mn} is the complex power flow from node m to n, and N is the number of nodes in the power network.

$$S_m = \sum_{n=1}^{N} S_{mn} \quad (8)$$

The complex power flow S_{mn} is expressed in (9) in terms of the complex nodal voltage V_m and V_n, and the line parameters.

$$S_{mn} = \frac{|V_m|^2}{\tilde{Z}_{mn}^*} - \frac{V_m V_n^*}{Z_{mn}^*} \quad (9)$$

Assuming that the line between two nodes is represented by a π equivalent circuit, Z_{mn} and Y_{mn} respectively indicate the series impedance and shunt admittance. Therefore, $\tilde{Z}_{mn}$ is

$$\tilde{Z}_{mn} = \left(\frac{1}{Z_{mn}} + \frac{Y_{mn}}{2}\right)^{-1} \quad (10)$$

C. Gas Networks

The gas injection to each node follows the conservation law of nodal gas flow balance. The mathematical formulations of the gas network are illustrated as follows [8], where the nodal gas flow balance for node m is

$$Q_m = \sum_{n=1}^{N} Q_{mn} \quad (11)$$

Where Q_m indicates gas injection to node m. Q_{mn} in (12) represents the gas flow between nodes m and n, which is expressed in terms of the upstream pressure p_m, downstream pressure p_n and k_{mn} depend on the pipeline's physical properties.

$$Q_{mn} = k_{mn} sn_{mn} \sqrt{sn_{mn}(p_m^2 - p_n^2)} \quad (12a)$$

$$sn_{mn} = \begin{cases} +1, & \text{if } p_m \ge p_n \\ -1, & \text{else} \end{cases} \quad (12b)$$

The gas consumed by compressors Q_{com} is formulated as

$$Q_{com} = k_{com} Q_{mn}(p_m - p_k) \quad (13)$$

Where k_{com} characterizes the properties of the compressor, p_m and p_k indicate the suction and discharge pressures at the two sides of the compressor. Specifically, gas power flow P_{mn} can be quantified by gas flow rate Q_{mn} and the gross heating value of gas (represented as GHV) as shown in (14).

$$P_{mn} = GHV \cdot Q_{mn} \quad (14)$$

III. Problem Formulation and Methodology

In a systematic way, the optimal operation normally consists of the following steps [7, 8, 11-13]:

i) the electricity load, heat load, and energy prices are normally forecasted by using historic data;
ii) the energy output of different generation is forecast, where the key uncertainties are the renewable generation;
iii) model the cost functions of all energy generation;
iv) model the operation objective function, and equality and inequality constraints for the optimization;
v) find an appropriate optimization approach to solve the model.

However, traditional deterministic methods fail to provide a reliable optimal solution because the renewable generation is assumed to be accurately forecasted. Chance-constrained programming enables the optimization of the system with the distributions of uncertain variables explicitly represented. By defining a probability level for the chance constraints, solving the CCP means to optimize the system with safety constraints and chance constraints satisfied, under the condition that the values of uncertainty variables are randomly distributed according to their distributions.

The impact of uncertain renewable generation on the energy hub system is modelled by chance constraints and the formulation of the optimization is presented in this section. Additionally, this section introduces the concept of Cornish-Fisher Expansion to convert chance constraints into deterministic constraints. The steps of the CCP implementation are at the end of this section.

A. CCP Energy Hub Optimization Problem Formulation

A system of three interconnected energy hubs in Fig. 2 is to illustrate the problem formulation. The electricity and gas networks supported by G1, G2, and N are embedded in the system to satisfy electricity and heat demand. G1 and G2 are generation power outputs, and N is the gas injection to the energy hub system. As shown in Fig. 2, heating converters including CHP, GSHP, and GF are installed within each hub, and a water tank is also contained in each hub as heat storage. A

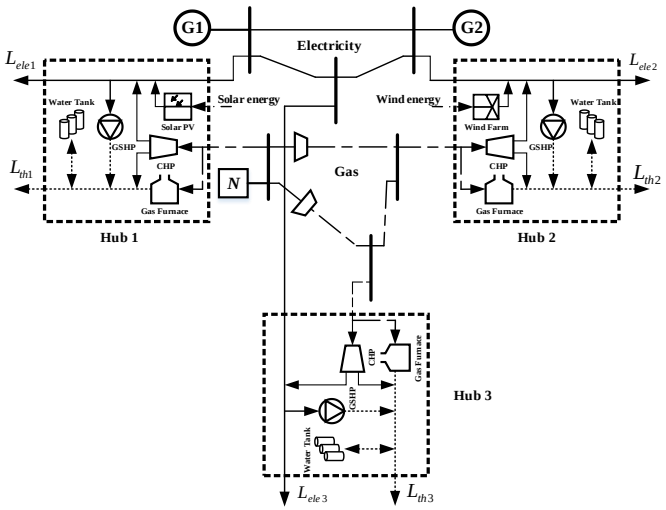

Fig. 2. The three-hub interconnected system.

solar photovoltaic system and a wind farm are installed at hubs 1 and 2 respectively.

The objective is to minimize the total system cost by optimally determining the power flow, gas flow, and the operation of each hub element over the whole operation time horizon with uncertain renewable. Meanwhile, the chance constraints on power and gas flows between adjacent hubs should be above the predefined probability level of confidence.

The optimal solution is denoted as the control vector *u(t)*, which contains the power and gas injection to the network and each hub, the voltage and pressure at each bus, the pressure of compressor, the power and gas flows between adjacent hubs, the energy exchange with the heat storage in each hub, and the dispatch factors for each hub. All these variables at all time-steps are included in the control vector *u(t)*.

$$u(t) = [P_{ele,i}(t), P_{gas,i}(t), V_i(t), P_{Gi}(t), P_N(t), S_{i,j}(t), p_i(t), Q_{i,j}(t), p_{com,i}(t), Mh_i(t), Eh_i(t), v_{e,i}(t), v_{g,i}(t)] \ \forall t, \forall i \quad (15)$$

In (15), '*i*' is the index number related to hubs, buses, nodes, and compressors. The definitions of other variables are in previous sections. The total cost (*TC*) of the electricity and gas generation is the objective to be minimized in terms of a quadratic function over whole time horizon *T*. It should be noticed that sn_{mn} in (12a) and (12b) is a binary variable, but it is temporarily used to calculate the gas flow Q_{mn} in (15). Hence sn_{mn} is not mentioned in the decision variables. The stochastic programming problem is formulated in (16).

Objective:

$$\text{Min } TC = \sum_{t=1}^{T} \sum_{i \in \{G_1, G_2, N\}} (a_{i,t} + b_{i,t} P_{i,t} + c_{it} P_{i,t}^2) \quad (16a)$$

Subject to:

Equality constraints: (1) − (14)

Inequality constraints:

$$0 \le v_{e,i}(t) \le 1 \quad 0 \le v_{g,i}(t) \le 1 \quad (16b)$$

$$0 \le P_{G,i}(t) \le P_{G,i,max}(t) \quad 0 \le P_N(t) \le P_{N,max}(t) \quad (16c)$$

$$0 \le P_{ele,i}(t) \le P_{ele,i,max}(t) \quad 0 \le P_{gas,i}(t) \le P_{gas,i,max}(t) \quad (16d)$$

$$0 \le p_i(t) \le p_{i,max}(t) \quad 0 \le V_i(t) \le V_{i,max}(t) \quad (16e)$$

$$M_{h,i,min}(t) \le M_{h,i}(t) \le M_{h,i,max}(t) \quad (16f)$$

$$E_{h,i,min}(t) \le E_{h,i}(t) \le E_{hi,max}(t) \quad (16g)$$

$$p_{com,i,min}(t) \le p_{com,i}(t) \le p_{com,i,max}(t) \quad (16h)$$

Chance constraints:

$$\Pr\{Q_{i,j}(t) \le Q_{i,j}^{max}\} \ge \alpha \quad \Pr\{S_{i,j}(t) \le S_{i,j}^{max}\} \ge \alpha \quad (16i)$$

The objective function in (16a) indicates the total cost on the network to be minimized over the whole time horizon, where a, b, and c represent the coefficient of generation cost. (16b) specifies the constraint on dispatch factors, which should be within the boundary between 0 and 1. (16c) indicates the constraint for total power and gas injection to the networks. (16d) reflects the minimum and maximum power and gas input to each hub. (16e) refers to the limitations of the pressure and voltage at each bus. (16f) denotes the limitation of heat energy exchange with the storage, the minimum and maximum heat energy that can be stored in the storage are defined in (16g). (16h) represents the limitation of compressor's pressure.

In addition to equality and inequality constraints, the chance constraints are also established with a confidence level of α. The power flows S_{ij} and gas flows Q_{ij} between adjacent hubs are constrained by chance constraints in this paper, and they are specified in (16i), where *Pr* means the probability of chance constraints.

Equation (16i) indicates that the problem is formulated as a stochastic problem. To transform the stochastic problem to a deterministic problem, the quantile of chance constraints is calculated by Cornish-Fisher Expansion to fit the optimization, and (16) is thus solvable with the interior-point method.

B. Transforming Chance Constraints to Deterministic Constraints

In order to incorporate chance constraints into the optimization, the probability level of chance constraints is transferred by quantile, which reflects the inverse function of a stochastic variable's Cumulative Distribution Function (CDF). Because of the monotone relation between the quantile and its inverse CDF, (16i) could be expressed by (17).

$$q_{Q_{i,j}}(\alpha_i) \le Q_{i,j,max} \qquad q_{S_{i,j}}(\alpha_i) \le S_{i,j,max} \quad (17)$$

Where q is the quantile function formulated by the Cornish-Fisher Expansion with the utilization of cumulants. Five orders of cumulants are applied in this paper. The quantile function q in terms of probability level of α is indicated in (18) [30].

$$q(\alpha) = A(\alpha) + \frac{A^2(\alpha)-1}{6}\kappa_3 + \frac{A^3(\alpha)-3A(\alpha)}{24}\kappa_4 - \frac{A^3(\alpha)-5A(\alpha)}{36}\kappa_3^2 + \frac{A^4(\alpha)-6A^2(\alpha)+3}{120}\kappa_5 - \frac{A^4(\alpha)-5A^2(\alpha)+2}{24}\kappa_3\kappa_4 + \frac{12A^4(\alpha)-53A^2(\alpha)+17}{324}\kappa_3^2 \quad (18)$$

The symbol A in (18) indicates the quantile of standard normal distribution, κ_v represents the cumulants with order *v*. It should be noted that the quantile q and cumulants κ_v follow the form of standard measure. For a variable q with a mean value of μ and standard deviation of σ, the normalized form of the variable and the cumulants are denoted as $q^* = (q-\mu)/\sigma$ and $\kappa_v^* = \kappa_v/\sigma^v$ respectively.

In order to calculate the quantile, the chance constraints need to be expressed in terms of uncertainty variables and other variables. Taking the chance constraint Q_{12} restricting the gas flow between hub 1 and 2 as an example, at each time step they are expressed by the composition of control variables *x* and uncertainty variables ξ, derived from (1)-(14). The chance constraint of Q_{12} at time step *t* is

$$Q_{1,2}(t) = a_1\xi_{solar}(t) + a_2\xi_{wind}(t) + Co(t) \quad (19)$$

Where, ζ_{solar} and ζ_{wind} stand for the uncertainty inputs of solar and wind energy respectively, a_1 and a_2 represent the coefficient related to ζ_{solar} and ζ_{wind}. Hence the two uncertain inputs perform linear relations with the variable gas flow between hub 1 and 2. Because the uncertain inputs to the energy hub system are linearly related to the chance constraints (power and gas flow between hubs), it is straightforward to obtain the linear relation in (19) through (1) - (14). *Co(t)* represents the polynomials containing control variables *x*, and it is irrelevant to the calculation of quantile. The first part in (19) related to the uncertainty inputs is expanded by the Cornish-Fisher Expansion to convert it to a deterministic formulation [30]. Assuming the uncertainty is abbreviated as *Un(t)*, the cumulant for *Un(t)* with order *v* is formulated in

$$\kappa_{Un(t),v} = a_1^v \kappa_{\xi_{solar,v}}(t) + a_2^v \kappa_{\xi_{wind,v}}(t) \quad (20)$$

Where $\kappa_{\xi_{solar,v}}(t)$ and $\kappa_{\xi_{wind,v}}(t)$ represent the cumulants of variables $\xi_{solar}(t)$ and $\xi_{wind}(t)$ with v^{th} order at time step *t*. The quantile of chance constraints can, therefore, be calculated through (18)-(20), and applied as the deterministic form in (17). The formulation of other chance constraints in (16i) can be accordingly transferred to deterministic constraints by the similar expressions shown in (18) to (20).

C. Overall Methodology

The methodology developed to solve the chance-constrained energy hub optimization is described by the following steps:

- Step 1. Acquire data: energy hub load, distributions of renewable generations, and system parameters.
- Step 2. Build the optimization problem with the given constraints, and chance constraints formulated in (16).
- Step 3. Initialize the control vector *u(t)* within the predefined boundary.
- Step 4. Convert the chance constraints into deterministic constraints through (17)-(20).
- Step 5. Apply the interior-point method to optimize the energy hub system with deterministic constraints.
- Step 6. Determine whether the solution from step 5 satisfies the stopping criteria, and if not, update the control vector *u(t)* and repeat steps 4 to 5 until the stopping criterion is met.

The optimization follows the general procedures of a heuristic algorithm, which is to update the optimal solution for the problem until the stopping criteria are met. However, as indicated in the previous section, the quantile of chance constraints not only depends on the probability level but also correlates with other control variables. Therefore, in updating the control variables, the chance constraints need to be circularly transferred to deterministic constraints at each iteration. The interior-point approach is then implemented to solve the deterministic problem to find the best solutions.

IV. EVPI AND VSS MODEL

To evaluate the effect of applying stochastic programming to solve the optimization problem, the results from the CCP are compared with those from the expected value of perfect information (EVPI) and value of the stochastic solution (VSS), both of which use deterministic programming to solve the optimization. The EVPI calculates the maximum amount a decision maker is willing to pay when uncertain information is perfectly known [31]. By assuming the uncertainty is modelled by various scenarios each with a known probability, the wait-and-see solution (WS) is derived by summing the optimal solution from each scenario multiplied by probability. The EVPI is calculated by (21), and SS is the solution from the CCP.

$$EVPI = SS - WS \quad (21)$$

The VSS reflects the benefits from explicitly modelling the uncertain distributions. It is mathematically formulated as the difference between the expected value (EV) of the optimal solution where uncertain variables are replaced by their mean values and the stochastic solutions [31].

$$VSS = EV - SS \quad (22)$$

V. CASE STUDY

The approaches of deriving PDF and CDF curves are illustrated in this section, and the convergence behaviour of the optimization technique is obtained and analysed by implementing the CCP on an example sample. Additionally, two cases are demonstrated and discussed in this section to validate the proposed model. The energy hub system in Fig. 2 is applied and the simulated time horizon is set as *T*=24. The chance constraints on gas and power flows between adjacent hubs are separately applied to the optimization problem in the first and second cases to investigate the impact of different chance constraints on system optimization performance. The system setup and data acquisition are indicated as follows.

A. Data Setup

The uncertainty in renewable energy generation, including solar energy and wind energy, are modelled in this paper. The CCP is used in this paper because a short period of overloading is tolerable for energy networks between communities, and hence a slight error is permissible.

Literature suggests that the characteristics of solar and wind energy generally follow Beta [30] and Weibull distributions [20]. Thus, the probability density functions of solar and wind energy injection at each time step are derived by fitting the historical data into Beta and Weibull distributions respectively, the shape factors of these distributions are then estimated. The

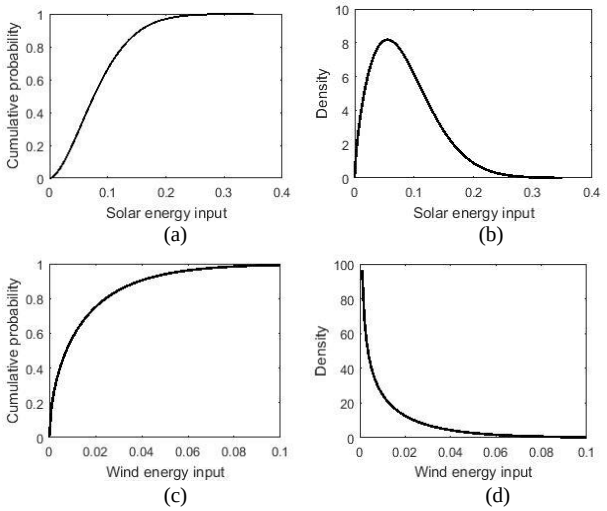

Fig. 3. PDF and CDF curves of renewable energies inputs at step 9

TABLE I
ENERGY HUB SYSTEM PARAMETERS AND CONSTRAINTS

System parameters	
Line 1-2	Z_{12}=0.3+j0.9 p.u., Y_{12}=j1.5·10^{-6} p.u.
Line 1-3	Z_{13}=0.2+j0.6 p.u., Y_{12}=j2.5·10^{-6} p.u.
Line 2-3	Z_{23}=0.1+j0.4 p.u., Y_{12}=j3.5·10^{-6} p.u.
G_1	V_1=1∠0^o, a_{G1}=0, b_{G1}=10 £/p.u., c_{G1}=0.001 £/p.u.^{2}
G_2	a_{G2}=0 b_{G2}=12 £/p.u., c_{G2}=0.0012 £/p.u.^{2}
Pipe lines	GHV·k_{12}=4.5 GHV·k_{13}=3.0 GHV·k_{23}=2.0
Compressor	GHV·k_{com}=0.5
N	p_1=1 p.u., a_N=0, b_N=5 £/p.u., c_N=0 £/p.u.^{2}
CHP	η_e=0.33, η_{gh}=0.57
GF	η_F=0.75
Storage	E_h^{stb}=0.5, e_h^+= e_h^-=0.9
Renewables	η_{so}=0.117, v_{ci}=4m/s, v_{co}=25m/s, v_{rs}=16m/s, P_{rated}=0.3p.u.
Constraints	
Nodes	0.8 ≤ $\|V_m\|$ ≤ 1.2 p.u.
m=1, 2, 3	p_m≤ 1.2 p.u.
G_2	0 ≤ P_{G2}≤4 p.u., 0 ≤ $\|Q_{G2}\|$ ≤ 4 p.u., 0 ≤ $\|P_{G2}+jQ_{G2}\|$ ≤ 5 p.u.
Compressor	1.2 ≤ p_m/p_k ≤ 1.8
Storage	0 ≤ E_h ≤ 6 p.u. -3 ≤ M_h ≤ 3 p.u.
CHP input	0 ≤ $P_{CHP,input}$ ≤ 1 p.u.
GF/GSHP	0 ≤ P_{GSHP/GF_input} ≤ 1.5 p.u.

cumulants are calculated based on the shape factors. The probability density function (PDF) curves and CDF curves of the solar and wind energy inputs at time step 9 are shown in Fig. 3 as an example. Here, figures (a) and (b) denote the characteristics of solar input, figures (c) and (d) indicate the wind input's PDF and CDF.

In addition to renewable uncertainties, the load profiles for the energy hub system are modelled by [32] and [33]. The parameters and constraints for other elements in the energy hub system are taken from [8, 13, 28], which are described in TABLE I. The system is considered as in a per unit (p.u.) system and the monetary unit is assumed to be GBP (£).

B. Derivation of PDF and CDF Curves

The results of CCP on the 3-hub system are analyzed with their PDF and CDF curves. All curves are sufficiently accurate to observe their characteristics when 500 samples are applied. The change to the curves are imperceptible when more samples are implemented, but the computational burden is exponentially heavy. Therefore, 500 samples are analyzed to acquire the PDF and CDFs plots. Generally, the two functions can be obtained by the following key procedures as shown in Fig. 4.

- Step 1: Implement the CCP optimization for the 3-hub system in terms of 500 samples, where each sample represents the CCP with different probabilities of chance constraints. For example, to acquire the PDF and CDF curves with chance constraint probability higher than 80%, the corresponding probability level of chance constraints equals to 80%+(n-1) *0.04% with n growing from 1 to 500.
- Step 2: Record the optimization results, including the optimal operations and objective value of each sample.
- Step 3: Build PDF and CDF curves by running 500 samples.

C. Case 1-Gas Flows with Chance Constraints

1) Convergence analysis of CCP

The optimization problem (16) is formulated as a multi-period problem, which is non-convex. Due to the high complexity of the problem, the global minimum is not guaranteed with the used interior-point method. However, the interior-point method is capable of resolving the non-linear

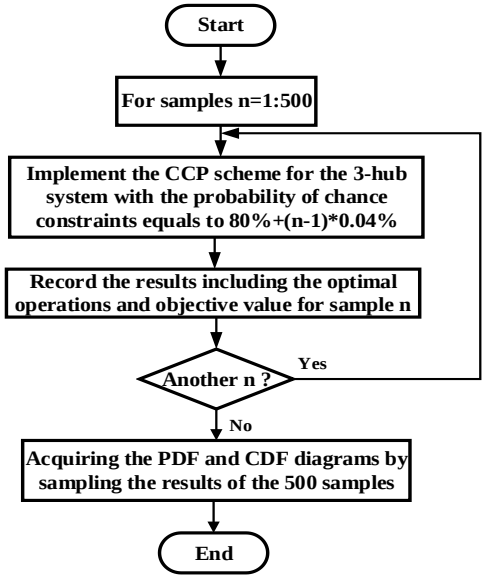

Fig. 4. Flowchart of obtaining PDF and CDF curves from CCP

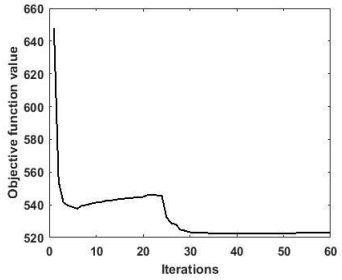

Fig. 5. The convergence of CCP implementing on the 3-hub system

problem compared with the linear programming methods. To demonstrate that the algorithm is capable of achieving a local minimum when applied to CCP, a single run of the 3-hub system is analyzed with the probability level of the chance constraints set as 80%, and the convergence behaviour of the optimization is derived and shown in Fig. 5. It can be seen that the value of the objective function dramatically declines from iteration 1 to 5. It then slightly increases until iteration 23, the curve continually drops from iteration 23 to 30, and remains stable thereafter. It demonstrates that the optimization converges around iteration 41 and achieves the minimum value of £522.33. It is, therefore, reasonable to conclude a local minimum has been met. In fact, the optimization converges for each sample after approximately 40 iterations. Additionally, previous literature has proved that the interior-point method applied to CCP is capable of converging to a minimum solution when solving problems with similar complexity [1, 8, 34].

2) Different probability levels of chance constraints

The maximum value of the chance constraint (i.e. the gas flow between adjacent hubs) is set as 0.8 p.u., and different probability levels of 80%, 85%, 90%, and 95% are applied to investigate how chance constraints affect the optimization.

The CDF curves of the optimized total cost are shown in Fig. 6, which are derived by optimizing 500 samples for the 3-hub system with the chance constraints level higher than the above probability levels. The optimized total costs of the three-hub system vary from approximately £521.5 to £527 with the cumulative probability changing from 0 to 1. All CDF curves perform similar characteristics with the optimization results derived from different chance constraint probability levels.

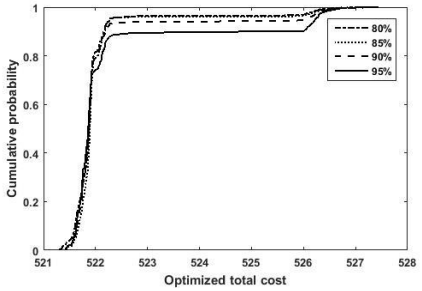

Fig. 6. Case 1-CDF curve of the optimized total cost

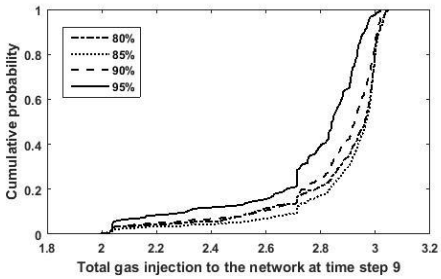

Fig. 7. Case 1-CDF curve of the total gas injection at time step 9

Since the load is relatively high at time step 9 compared to other time steps, the optimal operation for the energy hub at this time step is of interest for further investigation. The CDF curves of the total gas injection to the network at time step 9 with different chance constraints probability levels are in Fig. 7.

Fig. 7 indicates that all of the CDF curves gradually arising until the cumulative probability reaches 0.2, and then the curves rapidly increase to the cumulative probability of 1. The CDF curves with different probability levels of chance constraints present similar variation. The CDF curves in Fig. 7 present completely different characteristics with the CDF curves in Fig. 6. This is mainly due to the non-linearity between gas flow and the total system cost. Additionally, since the hub system presents high flexibility, the change of gas flows between hubs could lead to an unpredictable impact on the total cost. For example, the constraints on the quantity of gas flows could lead to less gas injection into the energy hub. The demand could be satisfied by accordingly adjusting the operations of other elements within the energy hub system such as discharging the storage or switching on other converters. Since the problem is a multi-period problem with high complexity, the cost of the adjustments is not predictable. Therefore, the CDF curves of the optimized total cost perform differently with the CDF curve of the gas flows between hubs.

D. Case 2-Power Flows with Chance Constraints

1) Different probability levels of chance constraints

The power flows between adjacent hubs are restricted by the chance constraints for the second case. Considering system safety limits, the maximum power flows between hubs are assumed to be 50% of branch capacity. With the different chance constraints probability levels of 80%, 85%, 90% and 95 %, the CDF curves of the total gas injection to the network at time step 9 are shown in Fig. 8, and the CDF curves of the optimized total cost are depicted in Fig. 9. 500 optimization results are sampled to derive the curves.

As seen from Fig. 8, the total gas injection at time step 9 varies from approximately 2.32 p.u. to 2.82 p.u.. The CDF

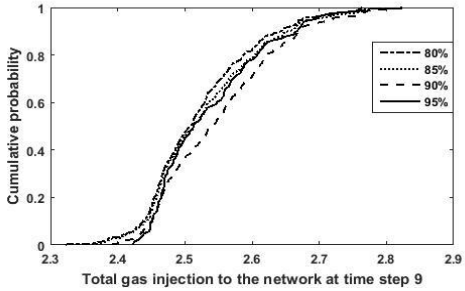

Fig. 8. Case 2-CDF curve of the total gas injection at time step 9

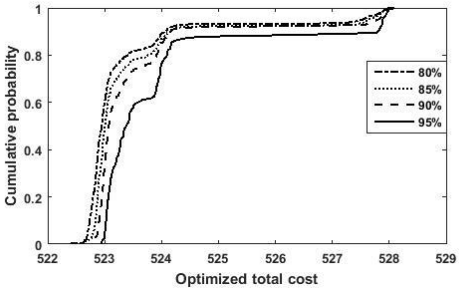

Fig. 9. Case 2-CDF curve of the optimized total cost

curve generally spans wider when the chance constraints probability level is lower, and the optimal operations tend to be more stable with fewer variations when the probability level of chance constraints is higher.

The characteristics of the CDF curves in Fig. 8 are different from the CDF curves in Fig. 7 in terms of shape and gradient. Additionally, the abscissa of the CDF curves in Fig. 7 spans from approximately 2 to 3, spanning greater distance compared with the CDF curves in Fig. 8. Hence the total gas injection to the network is more affected when the gas flows between hubs are restricted by the chance constraints.

Conversely, the CDF curves of the optimized total cost in Fig. 9 present similar characteristics with the curves in Fig. 6. However, the abscissa of the CDF curves in Fig. 9 spans wider than the curves in Fig. 6, which means that the optimized total cost is more sensitive when the power flows between hubs are constrained by chance constraints. Thus, when the restriction of chance constraints on gas flows change to power flows, the impacts to the optimal operations of every element within the energy hub system are completely different.

2) The optimal strategy for energy hub system

The optimal operation of hub 1 in terms of electrical load over 24 hours is shown in Fig. 10, where the probability levels of chance constraints are set higher than 80%. As seen, the total electrical load represented by the histogram and power injection to GSHP (denoted by stars) are met by the grid power

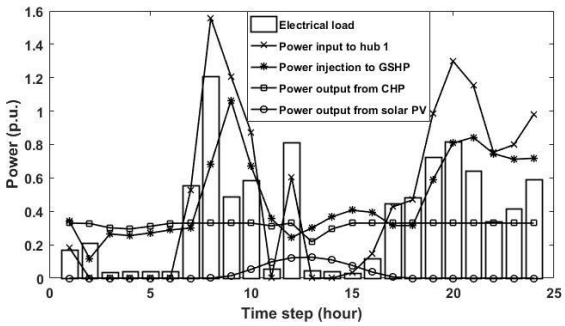

Fig. 10. Optimal strategy of hub 1 over 24 hours

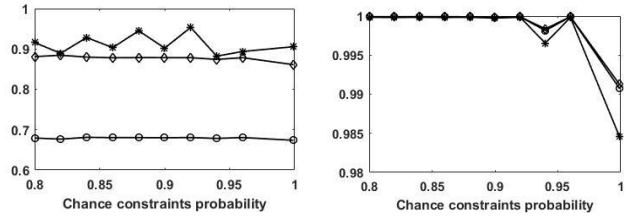

(a) (b)

Fig. 11. Dispatch factors under different chance constraints probability

(denoted by crosses), CHP output (denoted by squares), and solar PV output (denoted by circles). The peak loads are 1.21 p.u. and 0.92 p.u., which appear at time steps of 8 and 20; the power injections to the hub over 24 hours approximately follow the same variations as the load, and the maximum power injections are at time steps of 8 and 20 with the values of 1.55 p.u. and 1.30 p.u. respectively. The electric output from CHP generally remains at 0.33 p.u. over 24 hours, which is close to the maximum CHP power output. Since the energy efficiency of the CHP is higher than those of other converters and the CHP is thus more profitable, it is operated at the maximum power over the whole time horizon.

3) Sensitivity analysis

By assuming that the power flows between hubs are restricted by chance constraints, the probability levels of chance constraints are set to be 80%, 82%… to 99.9%. The optimal dispatch factors of the three hubs at time step 9 under these probability levels are shown in Fig. 11. Figures (a) and (b) indicate the variations of v_e and v_g under different chance constraint probabilities, with the horizontal and vertical axis representing the chance constraint probability and the value of dispatch factors. The diamonds, stars, and circles represent the dispatch factors of hubs 1, 2, and 3 respectively. As seen, the dispatch factors v_e of hubs 1 and 3 remain flat when the probability changes and the dispatch factor of hub 2 shows irregular variations. Moreover, the changing probability levels hardly affect the dispatch factors vg of the three hubs because the profits from the CHP are higher than those of the GF.

4) Importance of CCP

To highlight the importance of CCP and compare its results with those from deterministic approaches, EVPI and VSS are calculated by solving the same 3-hub system optimization with deterministic constraints. In other words, the maximum power flows between hubs are restricted to be lower than 50% of the capacity with 100% certainty. The value of WS is calculated by using scenario methods, where the probability of each scenario is assumed to be perfectly known. Scenario-generating methods are used in [5, 15-21], and hence the EVPI can be used to measure the impact between using CCP and scenario methods to solve an energy hub optimization problem with uncertainties.

In this paper, WS is derived by applying the 2PEM in [19, 20] to solve the energy hub optimization with uncertainties. In terms of system total cost, WS and EV are calculated as £524.02 and £522.92 respectively. The solution of CCP (SS) is £527.96 when the probability level of chance constraints is set at 99.99% (100% is not possible because the quantile derived through Cornish-Fisher Expansion will be infinite). The EVPI and VSS are £3.94 and £5.04 by using (21) and (22). The EVPI indicates that the difference between optimized system costs

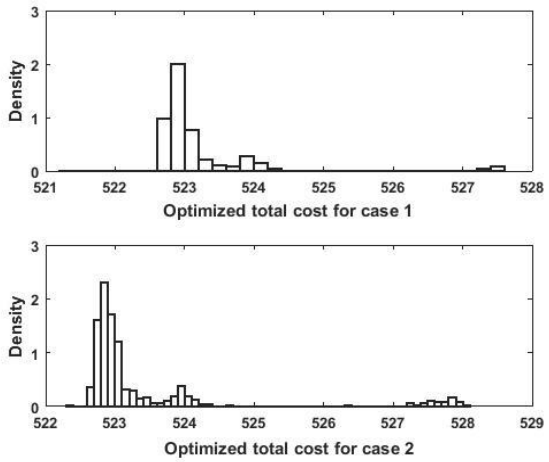

Fig. 12. PDF diagrams of the optimized total cost with the probability of chance constraints higher than 80% derived from the two cases

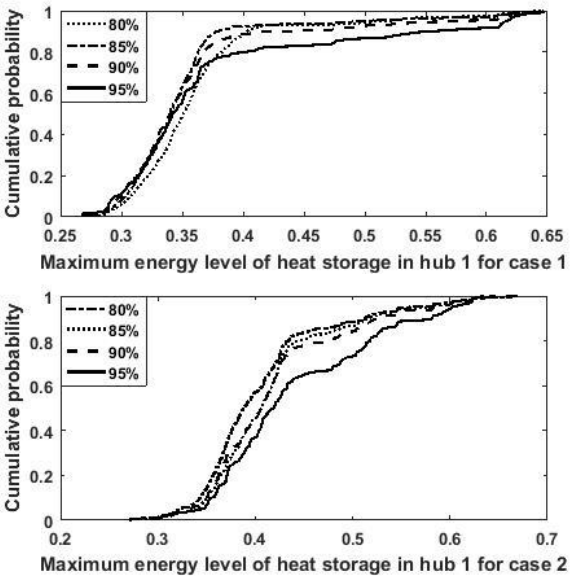

Fig. 13. CDF curves of Maximum energy level for two cases

from CCP and 2PEM is £3.94, and the VSS suggests that there is an extra cost of £5.04 due to uncertainties.

E. Comparison between the Two Cases

The PDF diagrams of the optimized objective derived from the two cases are shown in Fig. 12, where both the probability levels of chance constraints are set as 80%. The upper and lower diagrams represent the distributions of probability densities for case 1 and 2 respectively. The possible optimized total cost varies from £521.31 to £527.45 in case 1, and £522.39 to £528.10 in case 2. The span of the possible optimization results in case 1 is wider compared with the results derived from case 2. Additionally, the expense derived from case 2 is holistically higher than the expense in case 1.

It is observed from the lower diagram in Fig. 12 that, the PDF curve derived from case 2 presents relatively high fluctuations around £524 and £528 in addition to the high probability density around the total cost of £523. On the other hand, the probability density for the upper PDF curve is generally centralized around the total cost of £523, which shows stabilized characteristics. Therefore, by comparing the total

costs of the two cases, it suggests that the energy hub system tends to be more unstable and system cost is comparatively high when the power flows between hubs are restricted by chance constraints. Thus, the system should be carefully operated with the electricity power flows limited by chance constraints.

Since the heat storage is equipped within the energy hub system and optimized by CCP, the impacts of chance constraints to the operations of heat storages are investigated. The optimal operation of the heat storage in hub 1 is studied as an example. The energy level of heat storage quantifies the percentage of energy stored in it divided by its capacity, and the CDF curves of the maximum energy level of heat storage in hub 1 with different chance constraints probability levels are shown in Fig. 13. The upper and lower CDF curves are derived from case 1 and 2 respectively. As seen in Fig. 13, the CDF curves perform similar variation tendency for each individual case. However, the differences between the CDF curves in case 2 are more distinct compared to case 1, and the CDF curves have a broader span in case 2. It could be seen that the energy hub system tends to be more unstable when the chance constraints limit the power flows between hubs.

The results also suggest that the capacity of heat storage should be accordingly extended when the power flows between hubs are restricted by chance constraints since the maximum energy level in case 2 is higher than case 1.

VI. Conclusion

To model the intelligent operations of smart energy city with uncertainties, this paper applies the energy hub concept to optimize community renewable energy resources with uncertainty parameters. Chance-constrained programming is applied in this paper to solve the optimal energy flow problem for the energy hub system. The main findings are as follows:

- The uncertain elements of the energy hub system should be appropriately modelled since the stochastic nature can significantly affect energy hub system operations and costs.
- Chance-constrained programming is effective in optimizing energy hubs with uncertain factors, enabling the realistic operation of the energy hub system with minimum costs.
- Results demonstrate that chance constraints on power flows have a relatively high impact on energy hub system optimization. The results could be more unstable compared with the case of modelling gas flows with chance constraints.

Future work will incorporate other optimization schemes existing in smart energy cities, such as demand response and unit commitment by chance-constrained programming into the energy hub optimization. Additionally, the correlations of input random variables, such as wind outputs, will be considered as well by joint distributions in energy hub optimization.

References

[1] M. Geidl, "Integrated Modeling and Optimization of Multi-Carrier Energy Systems," *PhD dissertation, Power Systems Laboratory, ETH Zurich*, 2007.

[2] A. Sheikhi, M. Rayati, S. Bahrami, and A. M. Ranjbar, "Integrated Demand Side Management Game in Smart Energy Hubs," *IEEE Transactions on Smart Grid*, vol. 6, no. 2, pp. 675-683, Mar 2015.

[3] A. Sheikhi, S. Bahrami, and A. M. Ranjbar, "An autonomous demand response program for electricity and natural gas networks in smart energy hubs," *Energy*, vol. 89, pp. 490-499, Sep 2015.

[4] M. Geidl, G. Koeppel, P. Favre-Perrod, B. Klockl, G. Andersson, and K. Frohlich, "Energy hubs for the future," *IEEE Power & Energy Magazine*, vol. 5, no. 1, pp. 24-30, Jan-Feb 2007.

[5] F. Kienzle, P. Ahcin, and G. Andersson, "Valuing Investments in Multi-Energy Conversion, Storage, and Demand-Side Management Systems Under Uncertainty," *IEEE Transactions on Sustainable Energy*, vol. 2, no. 2, pp. 194-202, Apr 2011.

[6] S. Bahrami and A. Sheikhi, "From Demand Response in Smart Grid Toward Integrated Demand Response in Smart Energy Hub," *IEEE Transactions on Smart Grid*, vol. 7, no. 2, pp. 650-658, Mar 2016.

[7] M. C. Bozchalui, S. AhsanHashmi, H. Hassen, C. A. Canizares, and K. Bhattacharya, "Optimal Operation of Residential Energy Hubs in Smart Grids," *IEEE Transactions on Smart Grid*, vol. 3, no. 4, pp. 1755-1766, Dec 2012.

[8] M. Geidl and G. Andersson, "Optimal Power Flow of Multiple Energy Carriers," *Power Systems, IEEE Transactions on*, vol. 22, no. 1, pp. 145-155, 2007.

[9] M. R. Almassalkhi and A. Towle, "Enabling City-scale Multi-energy Optimal Dispatch with Energy Hubs," *2016 Power Systems Computation Conference (Pscc)*, 2016.

[10] C. C. Shao, X. F. Wang, M. Shahidehpour, X. L. Wang, and B. Y. Wang, "An MILP-Based Optimal Power Flow in Multicarrier Energy Systems," *IEEE Transactions on Sustainable Energy*, vol. 8, no. 1, pp. 239-248, Jan 2017.

[11] M. Moeini-Aghtaie, A. Abbaspour, M. Fotuhi-Firuzabad, and E. Hajipour, "A Decomposed Solution to Multiple-Energy Carriers Optimal Power Flow," *IEEE Transactions on Power Systems*, vol. 29, no. 2, pp. 707-716, Mar 2014.

[12] A. Shabanpour-Haghighi and A. R. Seifi, "Energy Flow Optimization in Multicarrier Systems," *IEEE Transactions on Industrial Informatics*, vol. 11, no. 5, pp. 1067-1077, Oct 2015.

[13] F. Adamek, M. Arnold, and G. Andersson, "On Decisive Storage Parameters for Minimizing Energy Supply Costs in Multicarrier Energy Systems," *Sustainable Energy, IEEE Transactions on*, vol. 5, no. 1, pp. 102-109, 2014.

[14] H. Yu, C. Y. Chung, K. P. Wong, and J. H. Zhang, "A Chance Constrained Transmission Network Expansion Planning Method With Consideration of Load and Wind Farm Uncertainties," *IEEE Transactions on Power Systems*, vol. 24, no. 3, pp. 1568-1576, Aug 2009.

[15] M. C. Bozchalui, C. A. Canizares, and K. Bhattacharya, "Optimal Energy Management of Greenhouses in Smart Grids," *IEEE Transactions on Smart Grid*, vol. 6, no. 2, pp. 827-835, Mar 2015.

[16] S. Chen, Z. N. Wei, G. Q. Sun, K. W. Cheung, and Y. H. Sun, "Multi-Linear Probabilistic Energy Flow Analysis of Integrated Electrical and Natural-Gas Systems," *IEEE Transactions on Power Systems*, vol. 32, no. 3, pp. 1970-1979, May 2017.

[17] B. M.-i. A. Dolatabadi, M. Abapour and S. Tohidi, "Optimal Stochastic Design of Wind Integrated Energy Hub," *IEEE Transactions on Industrial Informatics*, vol. 13, pp. 2379-2388, 2017.

[18] N. Neyestani, M. Yazdani-Damavandi, M. Shafie-Khah, G. Chicco, and J. P. S. Catalao, "Stochastic Modeling of Multienergy Carriers Dependencies in Smart Local Networks With Distributed Energy Resources," *IEEE Transactions on Smart Grid*, vol. 6, no. 4, pp. 1748-1762, Jul 2015.

[19] M. Rastegar, M. Fotuhi-Firuzabad, H. Zareipour, and M. Moeini-Aghtaie, "A Probabilistic Energy Management Scheme for Renewable-Based Residential Energy Hubs," *IEEE Transactions on Smart Grid*, vol. PP, no. 99, pp. 1-11, 2016.

[20] M. Moeini-Aghtaie, P. Dehghanian, M. Fotuhi-Firuzabad, and A. Abbaspour, "Multiagent Genetic Algorithm: An Online Probabilistic View on Economic Dispatch of Energy Hubs Constrained by Wind Availability," *IEEE Transactions on Sustainable Energy*, vol. 5, no. 2, pp. 699-708, Apr 2014.

[21] M. Alipour, K. Zare, and M. Abapour, "MINLP Probabilistic Scheduling Model for Demand Response Programs Integrated Energy Hubs," *IEEE Transactions on Industrial Informatics*, vol. 14, no. 1, pp. 79-88, Jan 2018.

[22] M. Wendt, P. Li, and G. Wozny, "Nonlinear chance-constrained process optimization under uncertainty," *Industrial & Engineering Chemistry Research*, vol. 41, no. 15, pp. 3621-3629, Jul 24 2002.

[23] G. Dorini, P. Pinson, and H. Madsen, "Chance-Constrained Optimization of Demand Response to Price Signals," *IEEE Transactions on Smart Grid*, vol. 4, no. 4, pp. 2072-2080, Dec 2013.

[24] H. Zhang and P. Li, "Chance Constrained Programming for Optimal Power Flow Under Uncertainty," *IEEE Transactions on Power Systems*, vol. 26, no. 4, pp. 2417-2424, Nov 2011.
[25] Z. Wu, P. L. Zeng, X. P. Zhang, and Q. Y. Zhou, "A Solution to the Chance-Constrained Two-Stage Stochastic Program for Unit Commitment With Wind Energy Integration," *IEEE Transactions on Power Systems*, vol. 31, no. 6, pp. 4185-4196, Nov 2016.
[26] J. Z. Liu, H. Chen, W. Zhang, B. Yurkovich, and G. Rizzoni, "Energy Management Problems Under Uncertainties for Grid-Connected Microgrids: A Chance Constrained Programming Approach," *IEEE Transactions on Smart Grid*, vol. 8, no. 6, pp. 2585-2596, Nov 2017.
[27] Q. F. Wang, Y. P. Guan, and J. H. Wang, "A Chance-Constrained Two-Stage Stochastic Program for Unit Commitment With Uncertain Wind Power Output," *IEEE Transactions on Power Systems*, vol. 27, no. 1, pp. 206-215, Feb 2012.
[28] M. Arnold, R. R. Negenborn, G. Andersson, and B. De Schutter, "Model-Based Predictive Control Applied to Multi-Carrier Energy Systems," *2009 IEEE Power & Energy Society General Meeting, Vols 1-8*, pp. 4592-4599, 2009.
[29] S. W. Xia, X. Luo, K. W. Chan, M. Zhou, and G. Y. Li, "Probabilistic Transient Stability Constrained Optimal Power Flow for Power Systems With Multiple Correlated Uncertain Wind Generations," *IEEE Transactions on Sustainable Energy*, vol. 7, no. 3, pp. 1133-1144, Jul 2016.
[30] M. Fan, V. Vittal, G. T. Heydt, and R. Ayyanar, "Probabilistic Power Flow Studies for Transmission Systems With Photovoltaic Generation Using Cumulants," *IEEE Transactions on Power Systems*, vol. 27, no. 4, pp. 2251-2261, Nov 2012.
[31] J. R. Birge and F. Louveaux, "Introduction to Stochastic Programming, Second Edition," *Introduction to Stochastic Programming, Second Edition*, pp. 3-+, 2011.
[32] I. Richardson, M. Thomson, D. Infield, and C. Clifford, "Domestic electricity use: A high-resolution energy demand model," *Energy and Buildings*, vol. 42, no. 10, pp. 1878-1887, Oct 2010.
[33] R. M. Yao and K. Steemers, "A method of formulating energy load profile for domestic buildings in the UK," *Energy and Buildings*, vol. 37, no. 6, pp. 663-671, Jun 2005.
[34] S. Paudyal, C. A. Canizares, and K. Bhattacharya, "Optimal Operation of Industrial Energy Hubs in Smart Grids," *IEEE Transactions on Smart Grid*, vol. 6, no. 2, pp. 684-694, Mar 2015.

Da Huo was born in Inner Mongolia, China. He received the B.Eng. degrees in electrical and electronic engineering from the University of Bath, U.K., and in electrical power engineering from North China Electric Power University, Baoding, China, in 2014. He is currently pursuing the Ph.D. degree with the University of Bath. His main research interests are multi-carrier energy system and smart grid.

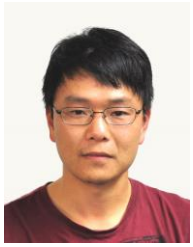

Chenghong Gu (M'14) was born in Anhui province, China. He received the Bachelor's degree from the Shanghai University of Electric Power, Shanghai, China, in 2003, and the Master's degree from the Shanghai Jiao Tong University, Shanghai, China, in 2007, both in electrical engineering. He received the Ph.D. degree from the University of Bath, U.K. He is currently a Lecturer with the Department of Electronic and Electrical Engineering, University of Bath. His major research interest is in multi-vector energy system, smart grid, and power economics.

Kang Ma (M'17) is now working as a lecturer at University of Bath. His research focuses on three-phase unbalanced low voltage networks. He worked as an R&D engineer at China Electric Power Research Institute (Beijing) from 2011 to 2014, during which time he developed the first version of the reliability assessment module for a distribution network planning platform. This platform has been widely applied to over 20 provincial grid companies in China. He received his PhD degree in Electrical Engineering from the University of Manchester (U.K.) and his B.Eng. degree from Tsinghua University (China).

Wei Wei was born in Gansu province, China. She received the Bachelor's degree from the University of Bath and North China Electric Power University in 2012, and the Master's degree from the University of Bath, in 2013, all in Electrical Power Engineering. She is currently pursuing the Ph.D. degree with the University of Bath, U.K. Her major research interest is in borehole thermal energy storage, renewable energy, and multi-energy system.

Yue Xiang (S'12-M'16) received the B.S. and Ph.D. degree from Sichuan University, China, in 2010 and 2016, respectively. Now he is an associate research professor in the College of Electrical Engineering and Information Technology, Sichuan University, China. His main research interests are power system planning and optimal operation, electric vehicle and renewable energy integration, and smart grids.

Simon Le Blond was born in Bath, UK and obtained his PhD in 2011 in power systems from the University of Bath in 2011. His main research interests are applying machine learning to energy storage, multiple energy carrier optimization and electrical power system protection.